Cartesian Impedance Control of Redundant Manipulators for Human-Robot Co-Manipulation

Fanny Ficuciello, Amedeo Romano, Luigi Villani, Bruno Siciliano

Abstract— **This paper addresses the problem of controlling a robot arm executing a cooperative task with a human who guides the robot through direct physical interaction. This problem is tackled by allowing the end effector to comply according to an impedance control law defined in the Cartesian space. While, in principle, the robot's dynamics can be fully compensated and any impedance behaviour can be imposed by the control, the stability of the coupled human-robot system is not guaranteed for any value of the impedance parameters. Moreover, if the robot is kinematically or functionally redundant, the redundant degrees of freedom play an important role. The idea proposed here is to use redundancy to ensure a decoupled apparent inertia at the end effector. Through an extensive experimental study on a 7-DOF KUKA LWR4 arm, we show that inertial decoupling enables a more flexible choice of the impedance parameters and improves the performance during manual guidance.**

I. Introduction

Robots that work close to people in their homes, offices or factories may be employed to support humans in the execution of certain types of tasks requiring intentional physical interaction, like helping in lifting and moving around heavy objects or tools, or performing cooperatively some operation, like assembling. During the execution of these tasks, the human guides the robot by exerting forces on some points of the robot's body, often the end effector, which should have a compliant behaviour. To be effective, this behaviour should be changed or adapted according to the task and, possibly, to human intentions. The control concept at the basis of robot compliance is the impedance control proposed by Hogan [1], which consists in imposing a desired dynamic behaviour to the robot, under the action of external forces, described by a second-order mechanical system of desired mass, damping and stiffness, together with a desired position trajectory, usually denoted "virtual" position. A compliant behaviour can be imposed to the robot's body as well [2].

In traditional robots, driven by stiff actuators, the impedance dynamics is obtained actively using control. On the other hand, intrinsically compliant robots have been built, with either elastic joints [3] or flexible links [5], [6]. More recently, robots driven by variable impedance actuators [7] have been conceived. With this new actuation technology, relying on passive compliant elements, it is possible to physically modify the stiffness and damping coefficients, thus resulting in higher energy efficiency, robustness, adaptability and safety with respect to traditional actuation.

Independently of the way the desired impedance behaviour is obtained, a crucial issue in human-robot cooperative tasks is the selection of the impedance parameters. These can be preset on the basis of the task to be executed, but a more effective solution consists in tuning the impedance behaviour of the end effector on the basis of the inferred human intentions [8], [9], [10].

Another important issue in implementing fixed or variable impedance control is that the stability must be guaranteed for all the possible range of variation of the parameters. The stability depends on the software, namely, how impedance control is implemented, but also on the hardware. These concern the robot kinematic structure, the robot dynamics, the transmission, the presence of friction, the kind of sensors and actuators [10], [16]. Furthermore, stability of human-robot interaction depends on the coupled dynamics of both interacting systems: even though the systems are stable in isolation, the coupled system may be unstable or perform inadequately.

Stability of impedance control has been largely investigated. Besides the seminal work of Hogan [1], stability problems have been discussed in [11], by using the concept of passivity, and in [12], where the concept of natural admittance control is introduced. Admittance and impedance are reciprocal concepts: while impedance control produces forces/torques in response to velocities, admittance control produces velocities in response to forces and torques, at a given interaction port.

The execution of tasks where the human drives the robot typically requires a low robot impedance, which should be further decreased when fast movements without particular precision are required and can be increased to perform fine motions. The structural impedance of general purpose robots, including commercial lightweight robots like the KUKA LWR4 arm, is usually higher than the ideal impedance required for an effective cooperation with humans. In particular, the equivalent inertia of the robot at the contact point (which hereafter is assumed to be the end effector) is often too high and must be reduced. This can be done by using feedback of the exchanged force. In this respect, it has been proven [11] that, by reducing the inertia more than 50% below its physical value, the system loses passivity, which is the property guaranteing stability when the robot interacts with any kind of passive environments. This limitation holds also for natural admittance control [12] which, with respect to impedance control, allows reducing friction

Dipartimento di Ingegneria Elettrica e Tecnologie dell'Informazione, Università degli Studi di Napoli Federico II, via Claudio 21, 80125 Napoli, Italy, email: {fanny.ficuciello, luigi.villani, bruno.siciliano}@unina.it, amedeo-havoc@gmail.com. This research has been partially funded by the EC Seventh Framework Programme (FP7) within SAPHARI project 287513 and RoDyMan project 320992.

and unmodelled dynamics, independently of inertia. On the other hand, several studies have shown, both theoretically and experimentally, that passivity may be too conservative and can be relaxed to improve performance [13], [14], [15].

This paper aims at contributing to this field by presenting an experimental study on impedance control of a redundant manipulator not specifically designed for human-robot cooperation, used for the execution of a drawing task under human guidance. The main purpose is to analyze if and how redundancy can be used to improve performance.

Starting from the consideration that instability is likely to occur during interaction when the controller attempts to impose to the robot an impedance dynamics that differs significantly from the intrinsic hardware dynamics, redundancy is exploited to make the robot apparent dynamics at the end effector as close as possible to the desired dynamics. In particular, since co-manipulation tasks typically require a decoupled impedance along the Cartesian directions, the redundant degrees of freedom are used to reduce as much as possible the dynamical coupling of the apparent inertia at the end effector.

The proposed control strategy has been tested on a case study where the human guides the end effector of a KUKA LWR4 in drawing a line along a predefined geometric path. Five different subjects, after some training, have been requested to execute the task with high precision. The results show that the use of redundancy to decouple the inertial dynamics of the end effector produces a tangible improvement of performance.

II. Impedance control with redundancy resolution

The KUKA LWR4 arm can be controlled, in principle, using impedance or admittance control. The two types of control have complementary pros and cons, that are well documented in the literature [17]. The algorithm considered here relies on impedance control with inertia reshaping.

The dynamic model of the robot has the form:

$$\boldsymbol{M}(\boldsymbol{q})\ddot{\boldsymbol{q}} + \boldsymbol{C}(\boldsymbol{q},\dot{\boldsymbol{q}})\dot{\boldsymbol{q}} + \boldsymbol{g}(\boldsymbol{q}) + \boldsymbol{\tau}_f = \boldsymbol{\tau}_c + \boldsymbol{J}^T(\boldsymbol{q})\boldsymbol{F}_{ext} \quad (1)$$

where $\boldsymbol{q} \in \mathbb{R}^n$, with $n = 7$, is the vector of joint variables, $\boldsymbol{M}(\boldsymbol{q})$ is the inertia matrix, $\boldsymbol{C}(\boldsymbol{q},\dot{\boldsymbol{q}})\dot{\boldsymbol{q}}$ is the vector of Coriolis/centrifugal torques, $\boldsymbol{g}(\boldsymbol{q})$ is the vector of gravitational torques, $\boldsymbol{\tau}_f$ is the vector of the friction torques, $\boldsymbol{\tau}_c$ is the control torque, $\boldsymbol{J}(\boldsymbol{q})$ is the robot Jacobian, and $\boldsymbol{\tau}_{ext} = \boldsymbol{J}^T\boldsymbol{F}_{ext}$ is the joint torque resulting from external force and moment $\boldsymbol{F}_{ext}$ applied to the end effector.

The control strategy is designed to perform tasks in cooperation with humans. The operator interacts with the robot by grasping the end effector and moving it along arbitrary trajectories. It is assumed that only forces can be applied. Hence, in (1), $\boldsymbol{F}_{ext}$ is the (3×1) vector of external force and $\boldsymbol{J}(\boldsymbol{q})$ is the (3×7) Jacobian relating the joint velocities to the end-effector translational velocity.

A. Impedance control

To design the impedance control, it is useful to derive the end-effector dynamics in the operational space [19], considering only the translational motion:

$$\boldsymbol{\Lambda}(\boldsymbol{q})\ddot{\boldsymbol{x}} + \boldsymbol{\mu}(\boldsymbol{q},\dot{\boldsymbol{q}})\dot{\boldsymbol{x}} + \boldsymbol{F}_g(\boldsymbol{q}) + \boldsymbol{F}_f(\boldsymbol{q}) = \boldsymbol{F}_c + \boldsymbol{F}_{ext} \quad (2)$$

where $\boldsymbol{x} \in \mathbb{R}^3$ is the Cartesian position vector, $\boldsymbol{\Lambda} = (\boldsymbol{J}\boldsymbol{M}^{-1}\boldsymbol{J}^T)^{-1}$ is the (3×3) end effector inertia matrix, hereafter denoted as apparent inertia, while $\boldsymbol{\mu}\dot{\boldsymbol{x}} = \boldsymbol{\Lambda}(\boldsymbol{J}\boldsymbol{M}^{-1}\boldsymbol{C} - \dot{\boldsymbol{J}})\dot{\boldsymbol{q}}$, $\boldsymbol{F}_g = \boldsymbol{J}^{\dagger T}\boldsymbol{g}$, $\boldsymbol{F}_f = \boldsymbol{J}^{\dagger T}\boldsymbol{\tau}_f$ and $\boldsymbol{F}_c = \boldsymbol{J}^{\dagger T}\boldsymbol{\tau}_c$ are the forces, reflected at the end effector, corresponding to the non-inertial joint torques in (1).

Equation (2) describes only the end-effector dynamics and does not include the so-called null space dynamics. Matrix $\boldsymbol{J}^\dagger$ is the dynamically consistent generalized inverse of matrix $\boldsymbol{J}$, defined as $\boldsymbol{J}^\dagger = \boldsymbol{M}^{-1}\boldsymbol{J}^T[\boldsymbol{J}\boldsymbol{M}^{-1}\boldsymbol{J}^T]^{-1}$. It can be proven that, only with this choice of generalized inverse, the null-space dynamics is not affected by the forces acting on the end effector [19].

Since the end effector has to follow and adapt to the force exerted by the operator at the tip, the end-effector dynamics can be set as a mass-damper system of equation

$$\boldsymbol{\Lambda}_d\ddot{\boldsymbol{x}} + \boldsymbol{D}_d\dot{\boldsymbol{x}} = \boldsymbol{F}_{ext}, \quad (3)$$

where $\boldsymbol{\Lambda}_d$ and $\boldsymbol{D}_d$ are suitable inertia and damping matrices, that here are set as constant diagonal matrices.

The above dynamics can be obtained in closed loop by choosing $\boldsymbol{F}_c$ in (2) as follows:

$$\boldsymbol{F}_c = \boldsymbol{\eta}(\boldsymbol{q},\dot{\boldsymbol{q}}) - \boldsymbol{\Lambda}(\boldsymbol{q})\boldsymbol{\Lambda}_d^{-1}\mathbf{D}_d\dot{\boldsymbol{x}} + (\boldsymbol{\Lambda}(\boldsymbol{q})\boldsymbol{\Lambda}_d^{-1} - \boldsymbol{I})\boldsymbol{F}_{ext}, \quad (4)$$

with $\boldsymbol{\eta}(\boldsymbol{q},\dot{\boldsymbol{q}}) = \boldsymbol{\mu}(\boldsymbol{q},\dot{\boldsymbol{q}})\dot{\boldsymbol{x}} + \boldsymbol{F}_g(\boldsymbol{q}) + \boldsymbol{F}_f(\boldsymbol{q})$.

The above equation is a Cartesian impedance control law with null stiffness and null virtual position. If the apparent inertia of the end effector is left unchanged, i.e., $\boldsymbol{\Lambda}_d = \boldsymbol{\Lambda}$, this equation does not depend on the external force $\boldsymbol{F}_{ext}$. Conversely, force feedback is required for inertia reshaping.

The external force can be measured by using a force/torque sensor mounted at the end effector. Alternatively, force estimation techniques can be adopted. An effective force estimation method, introduced in [18] is based on the generalized momentum $\boldsymbol{p}(t) = \boldsymbol{M}(\boldsymbol{q})\dot{\boldsymbol{q}}$ and the n-dimensional residual vector $\boldsymbol{r}$ defined as

$$\boldsymbol{r}(t) = \boldsymbol{K}_I\left[\int_0^t (\boldsymbol{\tau}_c - \boldsymbol{g}(\boldsymbol{q}) + \boldsymbol{r}(\sigma))d\sigma - \boldsymbol{p}(t)\right], \quad (5)$$

with $\boldsymbol{r}(0) = \mathbf{0}$, $\boldsymbol{K}_I$ a diagonal positive matrix and $\boldsymbol{p}(0) = \mathbf{0}$. The residual vector can be computed using measured signal $\boldsymbol{q}$, $\dot{\boldsymbol{q}}$ and the control torque $\boldsymbol{\tau}_c$. It can be shown that

$$\boldsymbol{r} \approx \boldsymbol{\tau}_{ext} - \boldsymbol{\tau}_\delta, \quad (6)$$

with $\boldsymbol{\tau}_\delta = \boldsymbol{C}(\boldsymbol{q},\dot{\boldsymbol{q}})\dot{\boldsymbol{q}} + \boldsymbol{\tau}_f$. Hence, multiplying from the left both sides of the above equation by $\boldsymbol{J}^{\dagger T}$ yields

$$\boldsymbol{J}^{\dagger T}\boldsymbol{r} \approx \boldsymbol{J}^{\dagger T}\boldsymbol{\tau}_{ext} - \boldsymbol{J}^{\dagger T}\boldsymbol{\tau}_\delta \approx \boldsymbol{F}_{ext},$$

where the contribution of friction torques and Coriolis and centrifugal effects reflected at the end effector has been

considered negligible with respect to the external force. Therefore, vector $\widehat{\boldsymbol{F}}_{ext} = \boldsymbol{J}^{\dagger T}\boldsymbol{r}$ is an estimate of the external force.

In view of the above approximations, the control law that imposes the impedance dynamics (3) can be implemented in the joint space in the form:

$$\boldsymbol{\tau}_{imp} = -\boldsymbol{J}^T\boldsymbol{\Lambda}[\dot{\boldsymbol{J}}\dot{\boldsymbol{q}} + \boldsymbol{\Lambda}_d^{-1}(\boldsymbol{D}_d\dot{\boldsymbol{x}} - \widehat{\boldsymbol{F}}_{ext})] + \boldsymbol{g}(\boldsymbol{q}) - \boldsymbol{r}. \quad (7)$$

B. Redundancy Resolution

In the presence of redundant degrees of freedom, which is the case considered here, it is possible to impose a secondary task in the null space of the end-effector task, according to the control law [19], [20]:

$$\boldsymbol{\tau}_c = \boldsymbol{\tau}_{imp} + (\boldsymbol{I} - \boldsymbol{J}^T\boldsymbol{J}^{\dagger T})(\boldsymbol{u} - k_D\dot{\boldsymbol{q}}), \quad (8)$$

where $-k_D\dot{\boldsymbol{q}}$, with $k_D > 0$, is a suitable damping torque and $\boldsymbol{u}$ is a torque vector to be designed, corresponding to a secondary task. This latter does not interfere with the main task, thanks to the use of the dynamically consistent projection matrix $\boldsymbol{I} - \boldsymbol{J}^T\boldsymbol{J}^{\dagger T}$.

In our application the human guidance of the end effector involves 3 of the 7 degrees of freedom of the robot, thus there are 4 degrees of freedom at disposal for the secondary task. Our aim is to use these additional degrees of freedom to improve the effectiveness of the main task, in terms of stability and human feeling.

Since it is well known that instability is likely to occur during interaction when the controller attempts to impose to the robot a dynamic behaviour that differs significantly from the intrinsic hardware dynamics (in particular, lower than the natural robot impedance), the idea pursued here is that of using redundancy to make the robot apparent dynamics at the end effector, described by (2) as close as possible to the desired dynamics (3).

The most critical element in (2) is the equivalent inertia, which is configuration dependent and cannot be decreased under a minimum value, depending on the robot kinematic structure and on the mass distribution. At any given end-effector position, what can be done is to exploit the internal motion to move the robot towards configurations with maximally decoupled inertia.

This can be achieved by using a task function inspired to the dynamic conditioning index (DCI) introduced by [21] to measure the dynamic isotropy of robot manipulators in joint space. In the operational space, the DCI index can be defined as the least-square difference between the generalized inertia matrix and an isotropic matrix, as:

$$\omega(\boldsymbol{q}) = -\frac{1}{2}\boldsymbol{E}(\boldsymbol{q})^T\boldsymbol{W}\boldsymbol{E}(\boldsymbol{q}) \quad (9)$$

where $\boldsymbol{W}$ is a diagonal weighting matrix and the error vector $\boldsymbol{E}(\boldsymbol{q})$ is defined as follows

$$\boldsymbol{E}(\boldsymbol{q}) = \begin{bmatrix} \lambda_{11}(\boldsymbol{q}) - \sigma(\boldsymbol{q}) \\ \lambda_{22}(\boldsymbol{q}) - \sigma(\boldsymbol{q}) \\ \lambda_{33}(\boldsymbol{q}) - \sigma(\boldsymbol{q}) \\ \lambda_{12}(\boldsymbol{q}) \\ \lambda_{13}(\boldsymbol{q}) \\ \lambda_{23}(\boldsymbol{q}) \end{bmatrix}, \quad (10)$$

being $\lambda_{i,j}(\boldsymbol{q})$ the generic element of $\boldsymbol{\Lambda}(\boldsymbol{q})$ and σ defined as

$$\sigma(\boldsymbol{q}) = \frac{1}{3}\mathrm{Tr}(\boldsymbol{\Lambda}(\mathbf{q})). \quad (11)$$

The maximization of $\omega(\boldsymbol{q})$ results in a minimization of the elements' norm of $\boldsymbol{E}$.

The weighting matrix $\boldsymbol{W}$ has been chosen in order to give priority to the minimization of the norm of the off-diagonal elements of $\boldsymbol{\Lambda}(\boldsymbol{q})$, i.e. $\boldsymbol{W} = \mathrm{diag}\{\boldsymbol{I}_3, 5\boldsymbol{I}_3\}$.

Finally, the control input $\boldsymbol{u}$ in (9) is chosen as

$$\boldsymbol{u} = k_c\left(\frac{\partial\omega(\boldsymbol{q})}{\partial\boldsymbol{q}}\right)^T, \; k_c > 0. \quad (12)$$

Fig. 1. Robot KUKA LWR4 in the configuration chosen for stability evaluation.

III. Stability region

An experimental procedure has been set up to find the allowed range of variation of the impedance parameters of (3) so that stability is preserved.

The stability region in the parameter space could be estimated analytically, by resorting e.g., to the concept of passivity as in [11] or complementary stability [13]. However, many authors have observed that the actual bounds of the stability region are dependent on the robot's hardware [10], [16] and, in the case of interaction with a human operator, depend on the impedance of the human arm, which cannot be accurately modelled and evaluated. In this work, the stability region in the parameter space has been found experimentally.

In the scalar case, Equation (3) can be rewritten in the Laplace domain as:

$$V(s) = \frac{1}{D}\frac{1}{1 + s\Lambda/D}F(s), \quad (13)$$

where V and F are the Laplace transforms of the velocity and force, respectively. Hence, it can be argued that the lower the damping, the higher the steady-state velocity for a given constant input force; moreover, for a given damping, the lower the inertia, the higher the bandwidth of the system or, equivalently, the lower the time constant Λ/D.

For the stability test, the joint configuration:

$$\boldsymbol{q}_0 = [0 \quad 0 \quad 0 \quad -90 \quad 0 \quad -45 \quad 0]^T,$$

represented in Fig. 1, has been selected. One reason for this choice is that, in this configuration, the end-effector inertia matrix is almost diagonal, and the designed control algorithm tries to keep $\boldsymbol{\Lambda}(\boldsymbol{q})$ as diagonal as possible during the task execution. Another reason is that, in this configuration, one of the eigenvalues of the inertia matrix (that corresponding to the vertical axis) assumes a value $\bar{\lambda}$ close to the maximum one, in the portion of the robot workspace where the task is executed. Hence, $\boldsymbol{q}_0$ is a worst case configuration for scaling the end-effector inertia.

The value of the inertia matrix in $\boldsymbol{q}_0$ and the corresponding vector of eigenvalues are

$$\boldsymbol{\Lambda}(\boldsymbol{q}_0) = \begin{bmatrix} 0.1187 & 0.0006 & 0.0226 \\ 0.0006 & 0.3069 & -0.1395 \\ 0.0226 & -0.1395 & 4.2405 \end{bmatrix},$$

$$\boldsymbol{\lambda}(\boldsymbol{q}_0) = [0.1186 \quad 0.3020 \quad 4.2456]^T.$$

To reduce the number of parameters, the same damping and the same mass have been set along all the directions of the Cartesian space, i.e., $\boldsymbol{D}_d = D\boldsymbol{I}$ and $\boldsymbol{\Lambda}_d = \Lambda\boldsymbol{I}$, with $\Lambda = \alpha\bar{\lambda}$, being $\bar{\lambda} = 4.2456\,\text{kg}$ the maximum eigenvalue and $0 < \alpha \leq 1$ a scaling factor. In this way, the desired impedance behaviour will be made isotropic by decreasing the mass along the vertical direction and increasing the mass values along the other two Cartesian directions which, therefore, are not critical for stability.

The stability region has been evaluated experimentally by setting a value of damping D in the interval $[5, 60]$ Ns/m and reducing the value of α, starting from $\alpha = 1$, until vibrations can be felt by an operator shaking the end effector in a neighbourhood of the initial configuration. The amplitude of the interval for the damping coefficient has been set on the basis of experiments where the natural robot's inertia was not modified.

The results of tests are reported in Fig. 2, where the stability region for the parameters D and α is that included between the blue line and the red line. It can be observed that any value of damping in the interval $[5, 60]$ can be chosen only if $\alpha > 0.25$ while, for $\alpha < 0.25$ the lower and upper bounds of the allowed damping become closer. For $\alpha < 0.1$ the robot starts vibrating for any value of damping.

A different representation of the same results is reported in Fig. 3, where the stability region is represented with respect to the time constant Λ/D of the impedance equation (13) and to the damping D. In this figure, two points of the stability region are evidenced: one corresponding to minimum damping (with minimum allowed time constant) and the other corresponding to maximum damping (with minimum allowed time constant). These values will be used in the experimental results presented in the next section.

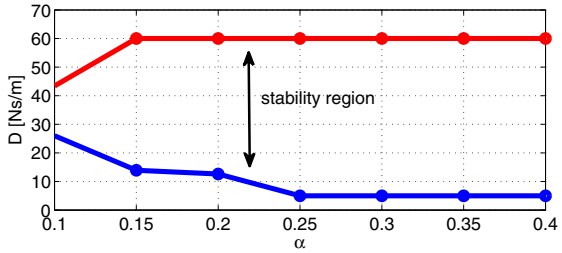

Fig. 2. Range of minimum and maximum allowed damping D for a given scaling factor α of the inertia matrix.

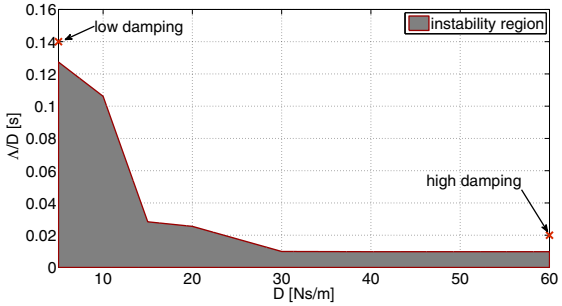

Fig. 3. Stability region: time constant Λ/D versus damping D

IV. Experiments

The experiments are aimed at showing the improvement in the performance that can be obtained with the proposed method of redundancy resolution.

The algorithm has been tested in the execution of a drawing task on a horizontal plane cooperated by a human. The operator guides a paint marker mounted on the robot's tip along a path drawn on a paper sheet. The path, represented in Fig. 4, has been designed with the aim of inducing trajectories with variable accelerations and is composed of long straight-line segments, sharp corners and smooth circular arcs.

The initial configuration of the robot, shown in Fig. 5 has been chosen to facilitate the execution of the drawing task planned on the horizontal plane and, at the same time, in correspondence with a local maximum of the DCI index. The latter choice avoids that the robot starts moving to reach a locally maximum isotropy configuration before the human operator begins to move the end effector.

The selected configuration is (joint angles in degrees):

$$\boldsymbol{q}_i = [2.35 \quad 22.8 \quad -1.54 \quad -53.2 \quad -3.1 \quad 101.15 \quad 0]^T,$$

with inertia matrix:

$$\boldsymbol{\Lambda}(\boldsymbol{q}_i) = \begin{bmatrix} 0.1265 & -0.0042 & 0.1470 \\ -0.0042 & 0.2002 & -0.0661 \\ 0.1470 & -0.0661 & 2.9396 \end{bmatrix}$$

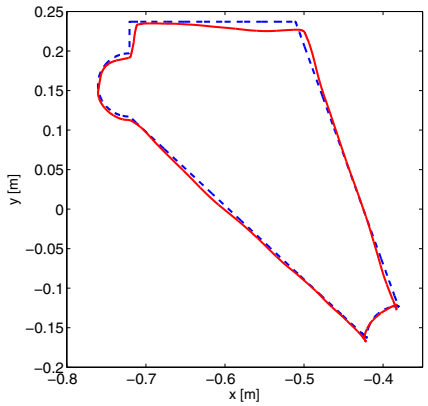

Fig. 4. Ideal path assigned for the drawing task (dotted line) and an example of execution (continuous line).

Fig. 5. Starting configuration for the drawing task.

and eigenvalues $\boldsymbol{\lambda}(\boldsymbol{q}_i) = (0.1188 \quad 0.1986 \quad 2.9489)^T$.

Two different sets of impedance gains are used, namely the high damping and the low damping gains represented in Fig. 3. Moreover, the experiments have been repeated with and without redundancy resolution. The algorithm without redundancy resolution have been implemented using setting $k_I = 0$ in (12).

The tests have been carried out on five different subjects using their dominant hand. A training phase, consisting in the execution of the compared strategies until the task was performed in a reasonable time (under 35 seconds) with all the control strategies, has been provided.

Since the assigned task consists in pursuing a given path, a fairly simple and effective method to measure the performance consists in comparing the length of the path drawn in cooperation with the robot, l_e, with the ideal path length, l_d, namely using the error $e = |l_d - l_e|$.

Another parameter is the execution time T of the trajectory, defined as the difference from the time when the entire path is completed and the time when the drawing tool touches the paper on the desk to start drawing.

In order to obtain measures that overcome the skills of the singular operator, the above parameters are evaluated as the average on the performance of the five subjects. During the experiments, the subjects were not informed about which strategies they were performing. In Fig. 6, the values of the

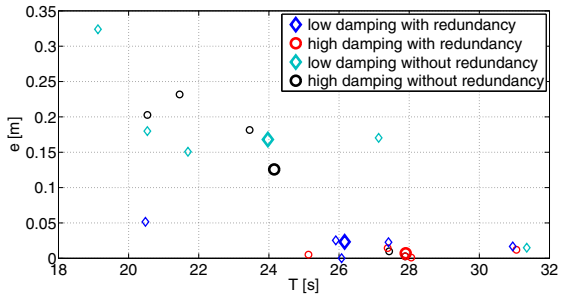

Fig. 6. Values of e and T in the experiments with low/high impedance with/without redundancy resolution. The bigger markers represent the mean values of five different subjects.

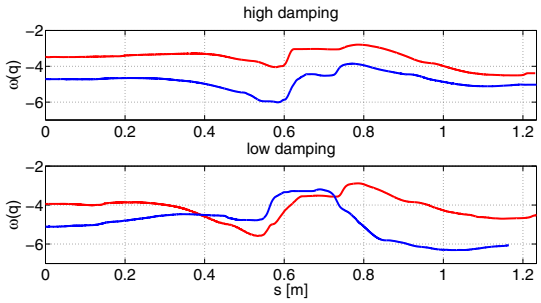

Fig. 7. Values of the dynamic conditioning index versus the curvilinear abscissa along the path, for the case of one subject. The red (blue) line represents the index value when redundancy is (not) used.

two parameters e and T are reported. It is possible to verify that, for both kinds of impedance, the control algorithms that uses redundancy overcomes the performance of the same algorithm without redundancy resolution in terms of error e. The execution time is slightly higher, especially in the case of high damping, but the difference was mainly due to the fact the operator was induced to increase the velocity to complete the task as soon as possible, due to the difficulty to keep high precision, especially in the final part of the task.

In Fig. 7 the trend of the dynamic conditioning index $\omega(\boldsymbol{q})$ in (9) is reported with respect to the path coordinate s (curvilinear abscissa). It is possible to observe that the length of the path is not always the same, since it depends on the error made by the cooperative human/robot system while drawing. Only the case of one subject has been represented.

For both the trajectories performed with high damping and low damping control, the figures show that, when the redundancy is exploited (red lines) the index is higher than in the case that redundancy is not used (blue lines). The blue line in the plot at the bottom of Fig. 7 has a shorter length. This is due to the fact that the task was not completed because the robot reached the configuration reported in Fig. 8, in which it was not possible to write anymore.

Figure 9 represents the norm of the linear forces exerted at the tip, for one subject, both in the case of high and low damping. The continuous lines are the corresponding mean values. As it is possible to observe, higher damping require higher forces to be exerted to execute the task. This leads to

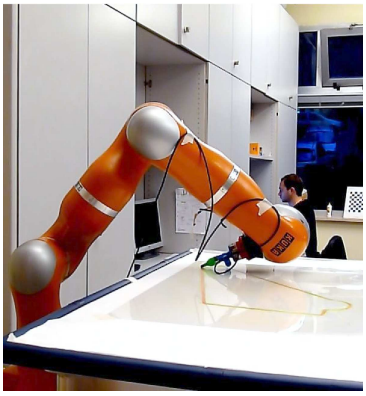

Fig. 8. Posture assumed during an experiment without the use of redundancy.

more precision, but higher execution time.

Extensive experiments have been made also using performance indices different from the dynamic conditioning index, e.g. the kinematic manipulability [4] or the dynamic manipulability index. The results of the experiments, that are not reported here for brevity, do not evidence significant improvement of performance with respect to the case that redundancy is not used. Last but not least, all the subjects involved in the experiments have found out that the "feeling" of the manual guidance (in terms of intuitiveness and response of the robot) improves when redundancy is used, as in this work, to decouple the natural end-effector dynamics along the principal directions of the task.

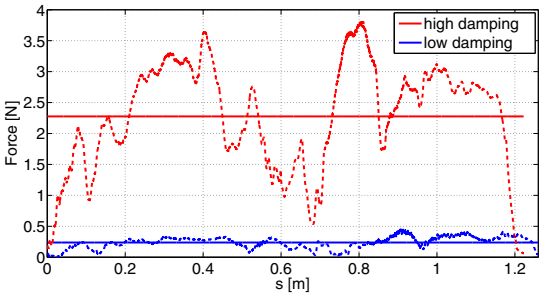

Fig. 9. Norm and mean value of the contact forces for high and low impedance, for the case of one subject.

V. Conclusions

In this paper, the problem of Cartesian impedance control of a redundant robot arm executing a cooperative task with a human has been addressed. In particular, redundancy has been used to keep robot's natural behaviour as close as possible to the desired impedance behaviour. This allows to easily find a region in the impedance parameter space where stability is preserved. Extensive experimental tests confirmed that this solution leads to better performance in the execution of a cooperative drawing task. The proposed method can be effectively extended to the case of variable impedance control, where the impedance parameters are modified on the basis of the interpretation of human intentions.

References

[1] N. Hogan, "Impedance control: An approach to manipulation: Part I theory; part II implementation; part III applications," *J. Dyn. Sys., Meas., Control*, vol. 107, no. 12, pp. 1–24, 1985.

[2] H. Sadeghian, L. Villani, M. Keshmiri, and B. Siciliano, "Task-space control of robot manipulators with null-space compliance," *IEEE Transactions on Robotics*, vol. 30, pp. 493–506, 2014.

[3] A. Albu-Schaffer, C. Ott, G. Hirzinger, "A unified passivity based control framework for position, torque and impedance control of flexible joint robots," *International Journal of Robotics Research*, vol. 26, pp. 23–39, 2007.

[4] F. Ficuciello, H. Sadeghian, L. Villani, and M. Keshmiri, "Global Impedance Control of Dual-Arm Manipulation for safe Human-Robot Interaction," *10th IFAC Symposium on Robot Control*, Dubrovnik, Croatia, 2012, pp. 767–773.

[5] B. Siciliano, and L. Villani, "Parallel force and position control of flexible manipulators," *IEE Proceedings: Control Theory and Applications*, vol. 147, pp. 605–612, 2000.

[6] B. Siciliano, and L. Villani, "An inverse kinematics algorithm for interaction control of a flexible arm with a compliant surface," *Control Engineering Practice*, vol. 9, pp. 191–198, 2001.

[7] B. Vanderborght, A. Albu-Schaeffer, A. Bicchi, E. Burdet, D. Caldwell, R. Carloni, M. Catalano, O. Eiberger, W. Friedl, G. Ganesh, M. Garabini, M. Grebenstein, G. Grioli, S. Haddadin, H. Hoppner, A. Jafari, M. Laffranchi, D. Lefeber, F. Petit, S. Stramigioli, N. Tsagarakis, M. V. Damme, R. V. Ham, L. Visser, and S. Wolf, "Variable impedance actuators: A review," *Robotics and Autonomous Systems*, vol. 61, no. 12, pp. 1601–1614, 2013.

[8] R. Ikeura, T. Moriguchi, and K. Mizutani, "Optimal variable impedance control for a robot and its application to lifting an object with a human," in *IEEE Int. Workshop on Robot and Human Interactive Communication*, Berlin, Germany, 2002, pp. 500–505.

[9] C. Mitsantisuk, K. Ohishi, and S. Katsura, "Variable mechanical stiffness control based on human stiffness estimation," in *IEEE International Conference on Mechatronics (ICM)*, Istanbul, 2011, pp. 731–736.

[10] A. Lecours, B. Mayer-St-Onge, , and C. Gosselin, "Variable admittance control of a four-degree-of-freedom intelligent assist device," in *IEEE Int. Conf. on Robotics and Automation*, Saint Paul, Minnesota, USA, 2012, pp. 3903–3908.

[11] J. Colgate and H. Hogan, "Robust control of dynamically interacting systems," *Int. J. of Control*, vol. 48, no. 1, pp. 65–88, 1988.

[12] W. Newman, "Stability and performance limits of interaction controllers," *ASME J, Dynamic Syst. Meas. Control*, vol. 114, no. 4, pp. 563–570, 1992.

[13] S. Buerger and N. Hogan, "Complementary stability and loop shaping for improved human-robot interaction," *IEEE Transactions on Robitcs*, vol. 23, no. 2, pp. 232–244, 2007.

[14] ——, "Relaxing passivity for human-robot interaction," in *IEEE/RSJ Int. Conf. on Intelligent Robots and Systems*, Beijing, China, 2006, pp. 4570–4575.

[15] V. Duchaine and C. Gosselin, "Investigation of human-robot interaction stability using Lyapunov theory," in *IEEE Int. Conf. on Robotics and Automation*, Pasadena, CA, 2008, pp. 2189–2194.

[16] V. Duchaine, B. Mayer-St-Onge, D. Gao, and C. Gosselin, "Stable and intuitive control of an intelligent assist device," *IEEE Transactions on Haptics*, vol. 5, no. 2, pp. 1939–1412, 2012.

[17] C. Ott, R. Mukherjee, and Y. Nakamura, "Unified impedance and admittance control," in *IEEE Int. Conf. on Robotics and Automation*, Anchorage, US-AK, 2010, pp. 554–561.

[18] A. D. Luca, A. Albu-Schäffer, S. Haddadin, and G. Hirzinger, "Collision detection and safe reaction with the DLR-III lightweight robot arm," in *IEEE/RSJ Int. Conf. on Intelligent Robots and Systems*, Beijing, China, 2006, pp. 1623–1630.

[19] O. Khatib, "A unified approach for motion and force control of robot manipulators: The operational space formulation," *IEEE Journal of Robotics and Automation*, vol. 3, no. 1, pp. 1115–1120, 1987.

[20] H. Sadeghian, L. Villani, M. Keshmiri, and B. Siciliano, "Dynamic multi-priority control in redundant robotic systems," *Robotica*, vol. 31, pp. 1155–1167, 2013.

[21] O. Ma and J. Angeles, "The concept of dynamic isotropy and its applications to inverse kinematics and trajectory planning," in *IEEE Int. Conf. on Robotics and Automation*, San Francisco, CA, 1990, pp. 10–15.